ACS APPLIED MATERIALS & INTERFACES

www.acsami.org

Research Article

Breathable, Self-Adhesive Dry Electrodes for Stable Electrophysiological Signal Monitoring During Exercise

Yan Liu, Yin Cheng, Liangjing Shi, Ranran Wang,* and Jing Sun*

Cite This: *ACS Appl. Mater. Interfaces* 2022, 14, 12812−12823

Read Online

ACCESS | Metrics & More | Article Recommendations | Supporting Information

ABSTRACT: On-skin electrodes with high air permeability, low thickness, low elastic modulus, and high adhesion are essential for biomedical signal recordings, which provide data for sports management and biomedical applications. However, nanothickness electrodes interacting with the skin by van der Waals force can be interfered with by sweating, and elastomers with high adhesion prepared by modification are not satisfactory in terms of air permeability. Here, a dry electrode with high stretchability (598%), low elastic modulus (5 MPa), high air permeability (726 g m^{-2} d^{-1}), and high adhesion (6.33 kPa) was fabricated by semi-embedding Ag nanowires into nonyl and glycerol-modified polyvinyl alcohol. Furthermore, a small amount of 40 wt % ethanol was sprayed on the skin to facilitate microdissolution of the substrate and form immediate conformability with skin texture. The dry electrodes can record high-quality electrocardiogram and electromyogram signals through a robust contact with the skin under skin deformation, with a water stream, or after running for 1 h. The film can also be served as the substrate for self-adhesive strain sensors to monitor motion with higher quality than nonadhesive polydimethylsilane-based sensors.

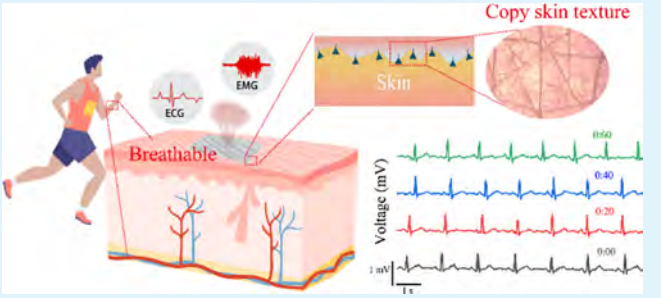

KEYWORDS: *electrophysiological detection, bioelectrodes, interfacial adhesion, gesture recognition, health monitoring*

INTRODUCTION

As the body's largest and outermost organ, human skin is an important medium for wearable electronics to collect physiological data,[1] such as temperature, pulse,[2] electrolyte level,[3,4] and electrophysiological signals.[5−10] Among them, electrophysiological signals play a significant role in disease diagnosis, rehabilitation medicine, sports monitoring, human−machine interaction, and other fields.[1,11−14] During real-time biomedical signal monitoring, the system of epidermal electronics is easier to operate compared to implantable electronics, but the signal amplitude from the epidermis is very weak because of the large impedance through the cuticle of the skin.[13] Therefore, electrodes that play an important role in directly implementing current conduction across the interface between the skin and the external circuit have attracted widespread attention.

Traditional Ag/AgCl gel electrodes have the limitations of skin irritation, gel dehydration, motion artifact, and failure in sweating. Therefore, on-skin electrodes that show high adhesion and good biocompatibility have become a focus in recent years.[15,16] Among those electrodes, the flexible resistive dry electrodes demonstrate a notable advance.[17−19] However, the morphology of the skin surface is complex and in dynamic change. For example, skin deforms almost all the time and excretes lots of sweat after exercising. Therefore, it is still difficult to maintain a robust contact between the skin and the electrode under skin deformation and a sweating state. According to the interface energy[20] interpreted as $U = U_{skin} + U_{bending} - |U_{adhesion}| < 0$ (U_{skin}: elastic energy of the skin; $U_{bending}$: bending energy of the electrode; and $U_{adhesion}$: interfacial adhesion energy), the realization of the conformal contact is dependent on low effective bending stiffness (Eh^3, E: Young's modulus and h: thickness) and high adhesion. For instance, electrodes with a thickness of hundreds of nanometers were fabricated using ultrathin elastic polymers, such as polydimethylsilane (PDMS), polyethylene terephthalate (PET), polyimide (PI), and styrene−ethylene/butylene−styrene (SEBS).[15,17,21−23] SEBS and PDMS have intrinsic low modulus and stretchability for conformal skin/electrode interfaces. Although the effective bending stiffness is markedly reduced by reducing the thickness, the adhesion energy based on van der Waals force between these materials and the skin is not high enough to assure a stable signal output during sweating or exercising. Jin-Hoon Kim used pure PDMS-based electrodes to test electrocardiogram (ECG) signals and no

Received: December 2, 2021
Accepted: February 21, 2022
Published: March 2, 2022

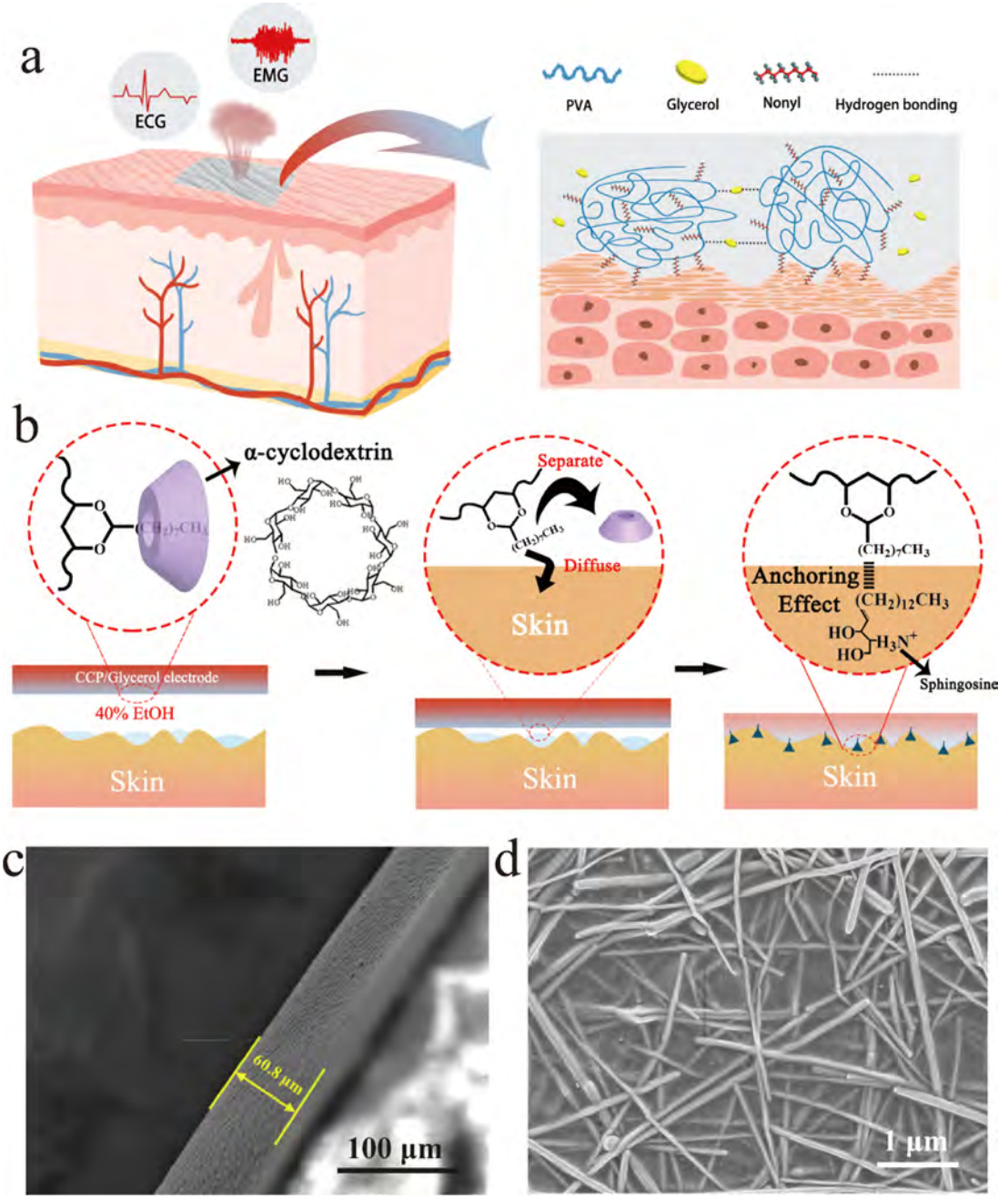

Figure 1. (a) Schematic illustration showing the conformal contact between the CCP/glycerol electrode and the skin. (b) Schematic illustration of the mechanism of adhesion between the CCP/glycerol film and the skin. (c) Cross-sectional SEM image of CCP/glycerol films. (d) Surface SEM image of Ag NWs distributed on the film.

complete P-QRS-T peaks were detected.[24] Moreover, high adhesion is a critical precondition for real-time health monitoring with the change of the service environment. Previous studies have attempted to fabricate highly adhesive elastomers. Xu and co-workers[25] obtained strong interfacial adhesion by incorporating dopamine groups into polyurethane segments, and electromyogram (EMG) signal monitoring under a sweating state was realized on this basis. Jin-Hoon Kim[24] introduced Triton X into PDMS to make it highly adhesive and compliant with the skin. Guo Ye[26] mimicked mussels and introduced dynamic disulfide bonds and hydrogen bonds into PDMS to confirm a stable interface contact with the skin. Unfortunately, these elastomers displayed unsatisfactory performance in terms of breathability, which may cause skin allergies during prolonged use. Hence, it seems to be a dilemma to achieve both good breathability and strong dynamic adhesion in a single electrode.

A polyvinyl alcohol (PVA) film is a material with good biocompatibility, biodegradability, and adhesiveness that is widely used as a carrier in biomedical engineering.[27,28] However, PVA is widely known as a semicrystalline polymer, in which intramolecular interactions and intermolecular interactions form a lot of hydrogen bonds,[29] so PVA films have high elastic modulus. In addition, the adhesion strength of PVA films relying on the interaction between alcohol hydroxyl and water molecules is disadvantageous when the skin sweats,

https://doi.org/10.1021/acsami.1c23322
ACS Appl. Mater. Interfaces 2022, 14, 12812−12823

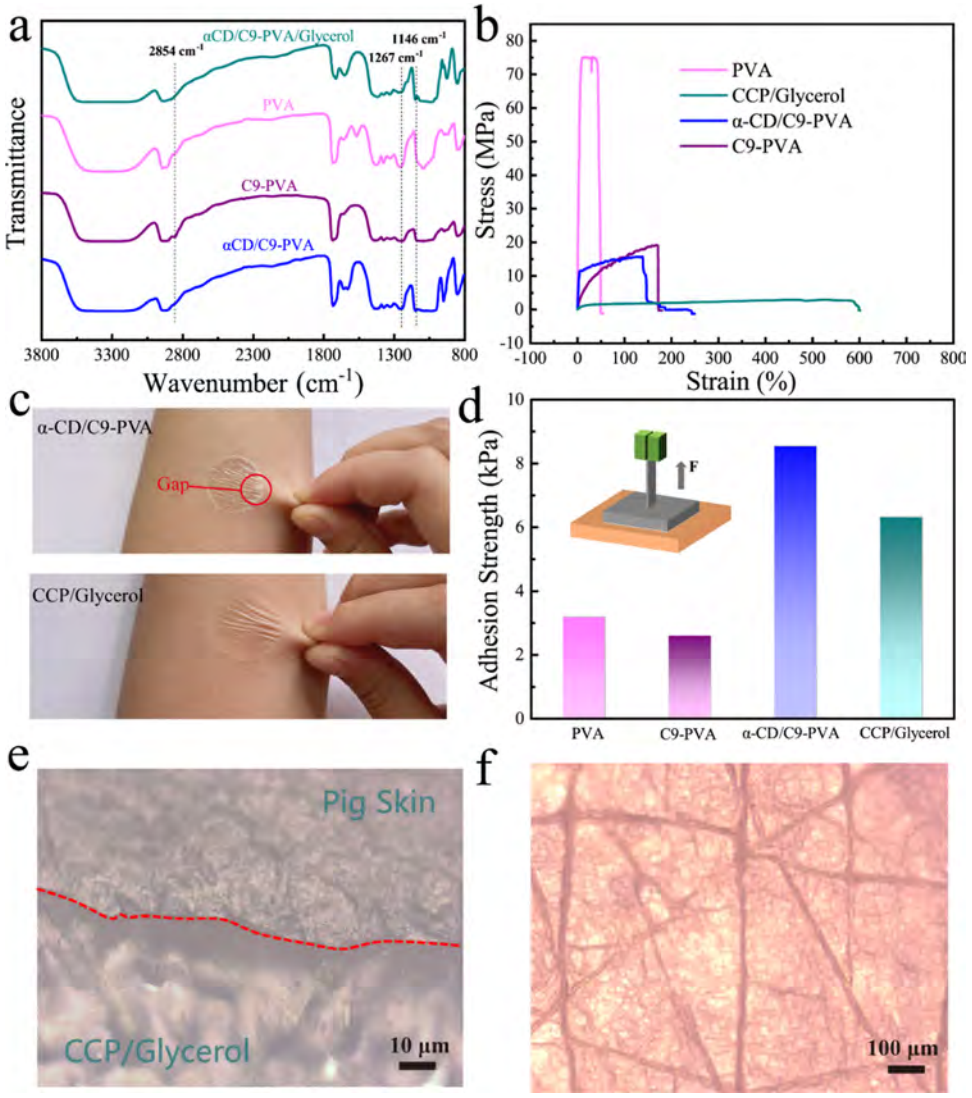

Figure 2. (a–d) Characterization of PVA films and modified PVA films. (a) FT-IR spectroscopy. (b) Stress–strain curves. (d) Tensile adhesion strength in the air. (c) Photo of α-CD/C9-PVA films and CCP/glycerol films under skin deformation. (e) Optical microscope images showing the interface between CCP/glycerol films and pig skin. (f) Optical microscope images of CCP/glycerol films after peeling from the skin.

which leads to poor water resistance and limits its application as wearable electronic substrates.

In this work, PVA films were functionalized to meet the requirements for mechanical properties in wearable devices. PVA was modified by a long alkyl chain nonyl with hydrophobicity, which was grafted onto the segment. An addition of glycerol was further introduced for plasticizing. Abovementioned modification reduced the elastic modulus of the film and enhanced the anchoring effect with skin. Therefore, the interfacial conformity between the film and the skin was improved under skin mechanical deformation and sweating. In addition, the air permeability of the film is about two times larger than PDMS with the same thickness. Ag nanowires (Ag NWs) with tensile resistant stability were spray coated as the interfacial conductive layer. This electrode exhibited more stable P-QRS-T peak output than the gel electrode in a cardiac cycle under skin tension and compression. It can also record stable ECG signals after 1 h of running. The root mean square (RMS) of the baseline noise of the electrode is smaller than that of a commercial Ag/AgCl gel electrode during recording EMG signals, and the signal-to-noise ratio (SNR) of the EMG signal for fisting can reach 15.42 dB. Additionally, compared with PDMS, the film can also be used as a substrate for strain sensing to detect motion signals with higher quality.

RESULTS AND DISCUSSION

Design and Characterizations of α-CD/C9-PVA/Glycerol Electrodes. We designed a robust contact between the PVA-based adhesive substrate and the skin, with a stable interface connection between the substrate and the conductive layer (Figure 1a). In the specific modification, nonyl groups were grafted onto PVA chains, forming six-membered rings that were supposed to enhance the film surface hydrophobicity and the anchoring effect with skin. However, the agglomeration of nonyl groups was found to hinder the improvement, therefore an amphiphilic substance, α-cyclodextrin (α-CD), was added to wrap nonyl groups (Figure 1b). Furthermore, glycerol was added to decrease the modulus of the α-CD/C9-PVA film by breaking the hydrogen-bonding force between long chain segments, so that it can better suit the dynamic adhesion needs of deformable skins. The thickness of the

https://doi.org/10.1021/acsami.1c23322
ACS Appl. Mater. Interfaces 2022, 14, 12812–12823

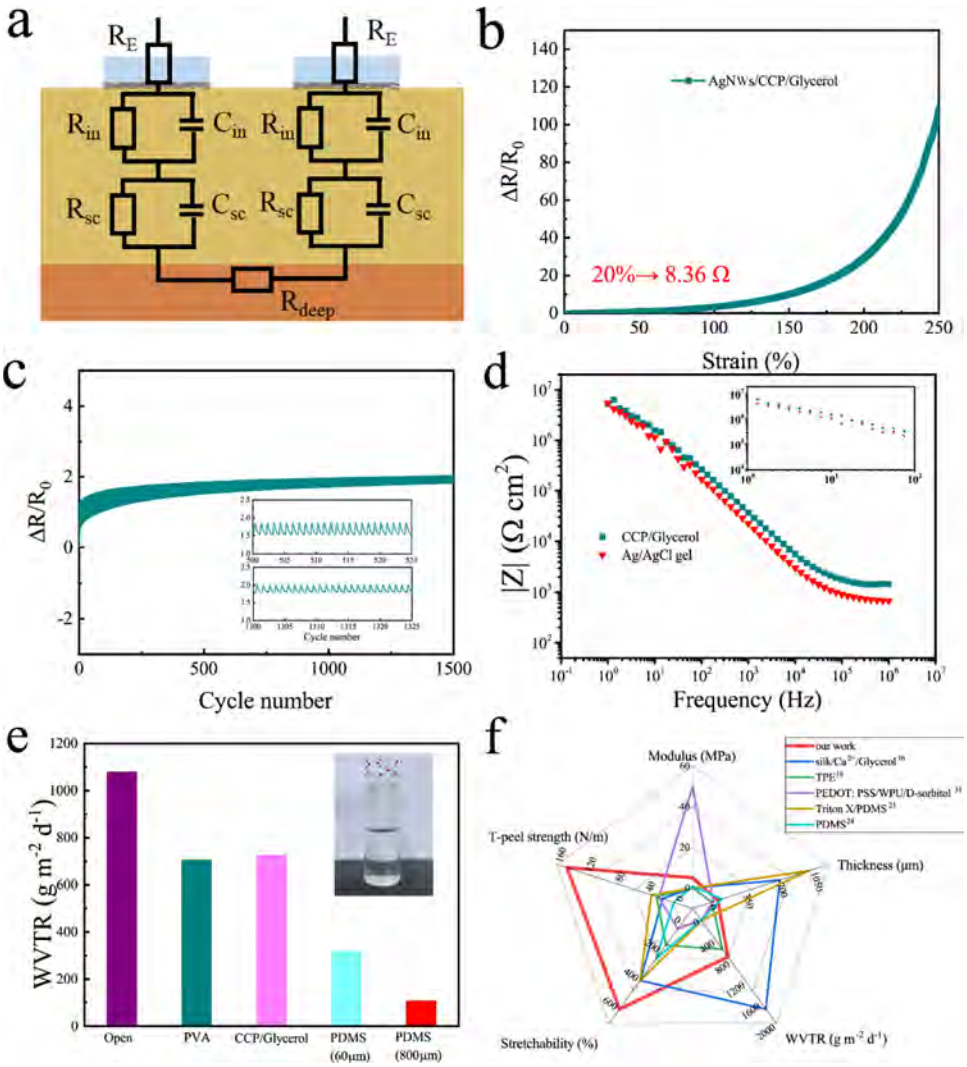

Figure 3. (a) Equivalent circuit model of the dry electrode when monitoring electrophysiology signals. (b) Resistance changes of Ag NWs on CCP/glycerol films under different tensile strains. (c) Cycle test of resistance change under 20% strain for 1500 laps. (d) Interface contact impedance between the skin and different electrodes. (e) WVTR of an open bottle sealed by different films with different thicknesses. (f) Radar plot for the properties of different on-skin electrodes.

CCP/glycerol substrate is about 50−60 μm (Figure 1c). Such thin films were prepared by drying a low-concentration solution in a mold and peeling them off. Atomization spraying was employed to deposit Ag NWs with an aspect ratio of 430 onto CCP/glycerol substrates to finish the fabrication of the dry electrodes. Ag NWs were randomly oriented and semi-embedded into the films, ensuring a robust combination between them (Figure 1d). This architecture was probably formed from the microdissolution of the film by ethanol on the interface. This interfacial bonding is very advantageous for the stable use of the electrode.[30] Similarly, a thin layer of 40 wt % ethanol was sprayed on the skin to improve the microdiffusion of α-CD/C9-PVA into the skin texture, which is favorable for the construction of high contact areas.

The structural characteristic peaks of PVA and modified PVA were revealed by the Fourier transform infrared (FT-IR) spectrum to explain the amelioration of mechanical properties and adhesion properties (Figure 2a). The peaks at approximately 2854 cm^{-1} (the C−H stretching vibration of αCH_2) and at approximately 1146 cm^{-1} (the absorption of C−O−C) confirmed the successful grafting of nonyl onto PVA segments.[31] Correspondingly, the stress−strain curves showed that C9-PVA films demonstrated an increased fracture strain (171%) and decreased tensile strength (19.15 MPa) compared to PVA films (49%, 74.9 MPa) with the same thickness (Figure 2b), which is due to the substitute for hydrogen-bonding forces from the oily group. However, the Young's modulus of C9-PVA films and α-CD/C9-PVA films was still very high (30, 313 MPa) and they are prone to producing relative displacement between the skin/electrode interface under mechanical deformations (Figure 2c top). When the loading of added glycerol was 28 wt %, the stress−strain curves indicated that the Young's modulus of CCP/glycerol films decreased to 5 MPa, while the strain at break increased to 598%. The decrease in the Young's modulus is favorable to the robust contact between the electrode and the dynamic deformable skin (Figure 2c bottom). The decreased modulus may originate from the reduced crystalline region that affects the movement of the polymer chain segment,[32] which was revealed by the decrease in intensity at the peak of 1267 cm^{-1} in the FT-IR spectrum and the larger peak width at 20° in the X-ray diffraction (XRD) spectra (Figure S1). Besides,

https://doi.org/10.1021/acsami.1c23322
ACS Appl. Mater. Interfaces 2022, 14, 12812−12823

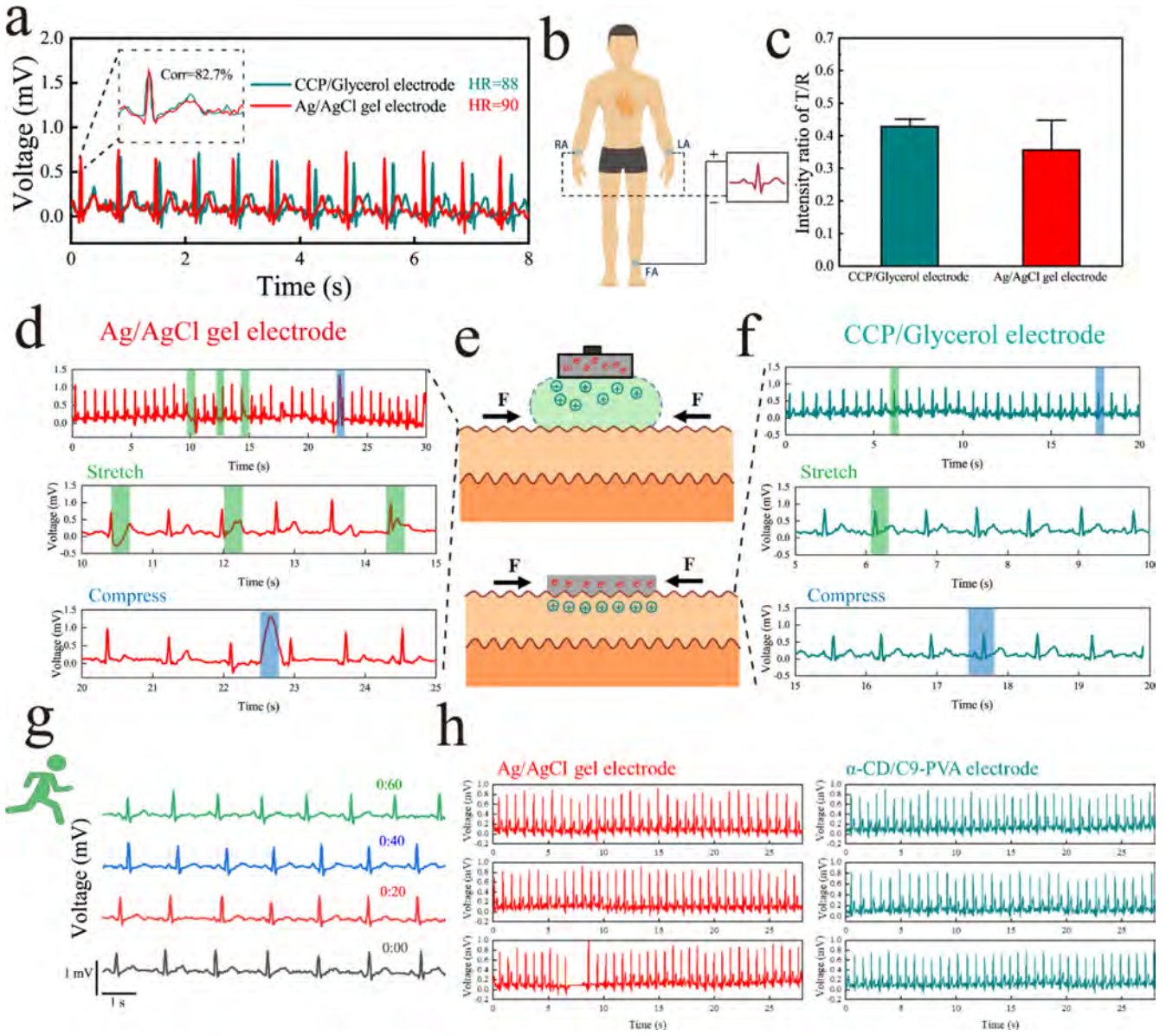

Figure 4. (a) ECG signals recorded by Ag/AgCl electrodes and CCP/glycerol electrodes through the (b) aVF positioning system. (c) T/R intensity ratio calculated from (a). (d–f) ECG signals monitored in a continuous period of time with applied force on the skin to cause stretching and compression. (g) ECG signals recorded from CCP/glycerol electrodes every 20 min for running for 1 h. (h) ECG signals recorded from Ag/AgCl electrodes and α-CD/C9-PVA electrodes at the beginning, middle, and end of the test for 28 s under a 15 min water stream.

compared to the flat and compact surface topography of PVA films as shown in scanning electron microscopy (SEM) images (Figure S2a,b), CCP/glycerol films presented a scaly terrain, which contributed to better stretchability because of the increase in the free volume. There is a slight increase in the Young's modulus (8 MPa) of the final device with the hindrance of silver NWs semi-embedded on the surface of thin films (Figure S3). In addition, CCP/glycerol films showed less strain loss compared to PVA films (2.58 and 7.42%) at a tensile strain of 20% in the first loading–unloading test, which indicated that the addition of glycerol increased the elastic region of the film (Figure S2c,d).

An interfacial tensile adhesion test perpendicular to pig skin was employed to characterize the adhesion strength, which is another requisite for the stability of the skin/electrode interface.[20] The adhesion strength of C9-PVA films is slightly lower than that of PVA films (2.6 and 3.52 kPa) (Figure 2d). There was supposed to be an enhancement of the adhesion strength of the skin when long alkyl chains were branched.[33] The aggregation of nonyl groups with each other can explain the failure of the interface interaction against expectations. The addition of α-CD, an amphipathic molecule which can form an inclusion with a long alkyl chain and separate easily by external interference (Figure 1b), increased the interfacial adhesion from 2.6 to 8.55 kPa. The enhancement in the adhesion strength could be attributed to the mechanical interlock between the film and the skin, the anchoring of nonyl to the skin, and the hydrophobic interaction with the epidermis, whose cuticle contains a large number of keratin and phospholipid bilayers. In detail, 40% EtOH made the film attached to the skin surface, and then water separated α-CD from nonyl and alcohol made the nonyl group free to anchor to the skin (Figure 1b). Additionally, the process of micro-dissolution also creates a mechanical interlock at the interface.

https://doi.org/10.1021/acsami.1c23322
ACS Appl. Mater. Interfaces 2022, 14, 12812–12823

The adhesion strength slightly declined to 6.33 kPa when more glycerol was added into the mixture, although there was still an obvious promotion compared to PVA films.

The intimate and robust contact between the skin/electrode interface can be verified by the establishment of a theoretical model in which the skin surface morphology is equivalent to a sinusoidal curve.[20] The requirement for conformal contact energy less than 0 is that the effective work of adhesion is bigger than 56.5 N/m (Supporting Information Note). The T-peeling strength between the CCP/glycerol film and the skin tested was 147 N/m and can meet the abovementioned requirement (Figure S4a,b). The optical microscope image showed that the film has compliance with pig skin in the interface region (Figure 2e). In addition, the surface topography of the film peeling from the skin showed the texture replication, which further proved the partial filling of the electrode into the skin indentation (Figure 2f).

Electrical Characterization. According to the equivalent circuit model between the skin/electrode interface during signal recording (Figure 3a), signal transducing qualities are not only determined by interface conformal contacts but also associated with the negligible conduction variation of the electrode under skin deformation.[24,25,34,35] The strain that skin responds to linear elastic tension is about 15% and at most 20%.[36] The resistance of Ag NW networks sprayed on CCP/glycerol films increased by 31% compared to original values under continuous tensile strain of 20% (Figure 3b). The signal processing device provided an input impedance of 10 GΩ and a common mode rejection ratio of 110 dB, which is tolerant of slightly increased noise caused by the little change in the resistance. The tensile cycling test at a strain of 20% was employed to evaluate the durability of CCP/glycerol electrodes in resistance (Figure 3c). Because the film cannot completely return to the initial position after stretching, the resistance value increased to about three times at the initial 500 cycles. In the last 1000 cycles, the resistance stabilized at 19.02 Ω and the low values ensured surface biopotential recordings even under the continuous deformation of the skin.

The low skin/electrode interface contact impedance is a prerequisite for as a small loss of voltage as possible,[37] and a small change in the skin contact impedance will lead to a large variation in potential, which will further cause skin motion artifacts or signals out of range.[38−40] The interfacial contact impedances of CCP/glycerol electrodes and commercial Ag/AgCl gel electrodes, which excluded the influence of the area, were measured in the frequency range of 1−10^6 Hz (Figure 3d). The measured results are consistent with the range of previous research results.[41] We paid special attention to the impedance values in the low-frequency region (EMG: 10−500 Hz and ECG: 0.5−100 Hz).[42] The interfacial impedance of CCP/glycerol electrodes is comparable to that of commercial gel electrodes at 10 Hz (1217 and 1139 kΩ cm^2), indicating the feasibility of testing electrophysiological signals. Furthermore, the interface contact impedance values of PVA electrodes and CCP/glycerol electrodes under static and dynamic states were compared to verify the modification effect (Figure S5). The contact impedance of CCP/glycerol electrodes increased by 22 and 15% under stretch and compression states separately, while that of PVA electrodes increased by 100 and 88%, respectively, obviously demonstrating that CCP/glycerol electrodes have better anti-interference behavior in the circumstances of skin deformations. The lower Young's modulus and higher adhesion strength of the CCP/glycerol film are mainly responsible for this improvement.

The permeability of water vapor is essential for wearable electrodes to avoid body discomfort and skin irritation during long-term use.[43] The water vapor transmission rate (WVTR) of the CCP/glycerol film is 726 g m^{-2} d^{-1} (Figure 3e), which is slightly better than pure PVA films and approximately twice as large as that of the PDMS film (400 g m^{-2} d^{-1}) with the same thickness (60 μm), which is widely used as an elastic substrate in on-skin devices. This can be explained by the fact that although the polymer segments in the PDMS elastomer are flexible, the CCP/glycerol blend, which makes a balance between hydrophobicity and hydrophilicity, contains lots of hydroxyl groups and shows high affinity for water molecules despite the grafted nonyl and is in favor of the dissolution and diffusion of water molecules. In addition, the decrease in crystallinity also provides favorable conditions for the penetration of water molecules (Figure S1) because that will provide a larger free volume for molecules to diffuse.[44] The radar plot for the properties of different on-skin electrodes revealed performance advantages in our work (Figure 3f). The data of Figure 3f are shown in Table S1. Moreover, CCP/glycerol electrodes can be healed by spraying 40 wt % ethanol to light the extinguished bulb (Figure S6), which can avoid short circuits caused by self-healing.[45]

Electrocardiogram Signal Monitoring. The rule of spatial distribution of electrodes for ECG signal recording (Figure 4a) is augmented by unipolar limb leads—aVF (Figure 4b).[46] The electrodes were cast in the shape of a circle and the procedure for placing them on the skin is shown in the Experimental Section. Ag NWs prepared by spraying showed a semi-embedded morphology on the substrate, resulting in a slight decrease in the overall adhesion strength, but still maintaining a high value (Figure S7a). In addition, the adhesion process does not destroy the silver NW network, so the resistance of the electrodes does not increase significantly after being stripped from the skin (Figure S7b). Thus, the P-QRS-T band corresponding to a cardiac cycle can be clearly observed from the waveform. Signals collected from CCP/glycerol electrodes and Ag/AgCl gel electrodes were analyzed to compare the average heart rate (88, 90), both of which were within the normal range (60−100). The Pearson correlation coefficient (corr) is used to describe the similarity of two curves.[47] The corr of two curves is 82.7%, showing the high similarity between the two electrodes. In addition, the voltage intensity ratio of the T wave to the R wave was defined to compare the sensitivity of different electrodes.[30] The intensity ratio of T/R of our electrodes is higher than that of Ag/AgCl electrodes (Figure 4c), which shows the potential for heart disease diagnosis. The commercial Ag/AgCl gel electrode is supported by a rigid substrate, and the double capacitive layer between the electrode−electrolyte interface will be disturbed if the skin deforms,[40] and it will further lead to poor signal output with disordered charge distribution (Figure 4d,e top). Continuous ECG signal recording indicated that when stretching or compressing the skin, signal corruption in a cardiac cycle can be clearly observed. The ST band has a completely horizontal downward shift or a hunched upward lift (middle), and the P wave voltage value exceeds the general range (0.25 mV, bottom), which will mislead judgments about myocardial ischemia and right atrial hypertrophy, respectively. The projection of ECG signals has little change under tension and compression conditions for CCP/glycerol electrodes (blue

https://doi.org/10.1021/acsami.1c23322
ACS Appl. Mater. Interfaces 2022, 14, 12812−12823

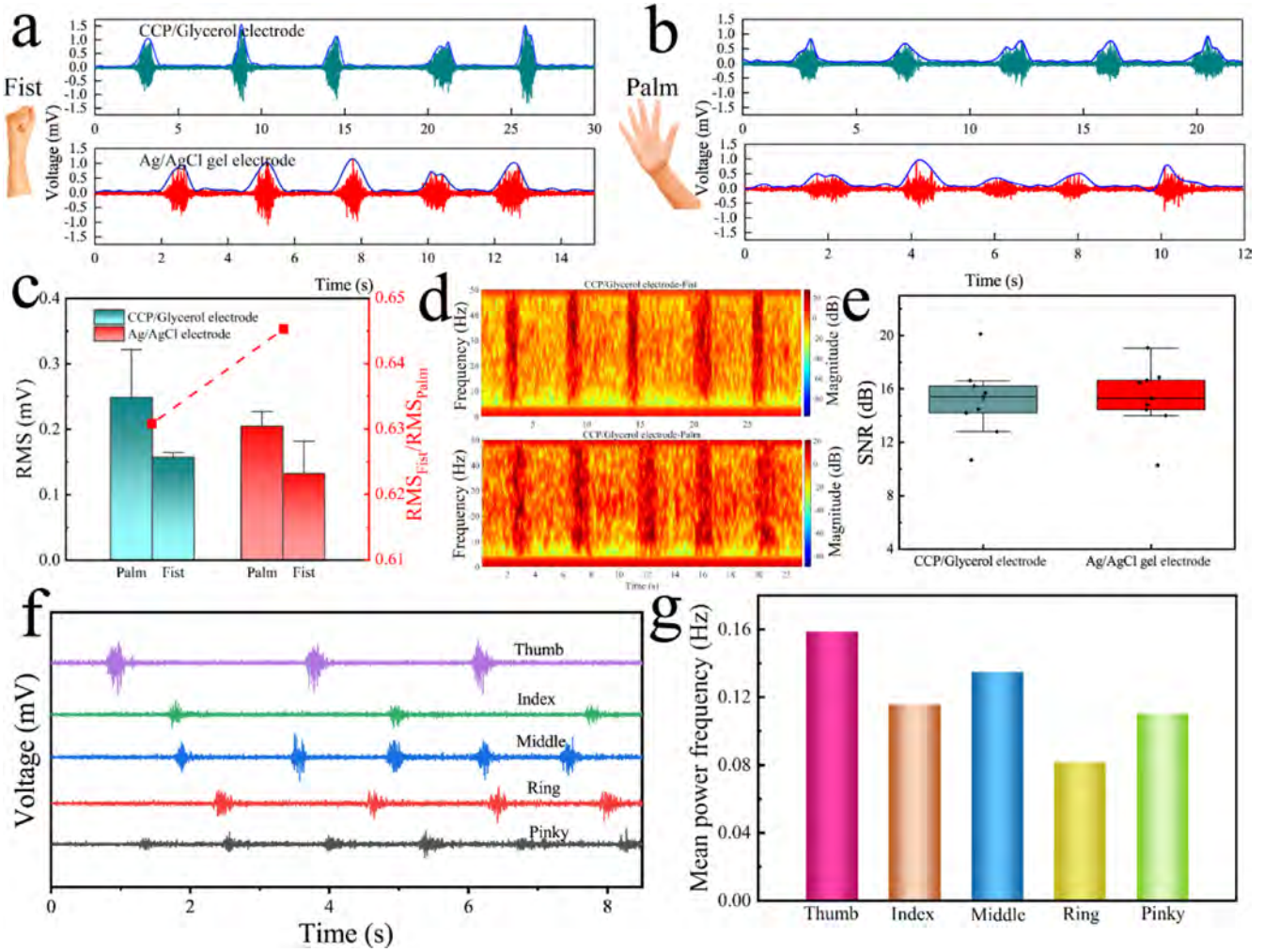

Figure 5. (a,b) Measurement of EMG signals produced by fisting and palm through CCP/glycerol electrodes (a) and commercial Ag/AgCl gel electrodes (b) at the same position with similar force and speed. (c) RMS values calculated from (a,b). (d) Spectrogram of EMG signals monitoring the motion of fisting (left) and palm (right) by CCP/glycerol electrodes. (e) SNR of different bands from EMG signals of nine different actions. (f,g) EMG signals (f) of actions corresponding to different fingers and the extracted mean power frequency (g).

and green areas in Figure 4f), which originates from the more stable contact potential of dry electrodes (Figure 4e bottom). Moreover, CCP/glycerol and α-CD/C9-PVA films exhibited raised hydrophobicity with nonyl grafting according to the increased water contact angle (Figure S8a). Therefore, it can be seen that the film has high adhesion strength under high humidity in Figure S9. The improvement in water resistance provided the possibility for underwater use for a short time. The CCP/glycerol electrodes can record the stable surface biopotential every 20 min during the volunteer's runs for 1 h with sweating (Figure 4g). Moreover, the ECG signals of walking for an hour have been displayed in Video S1. The change of underwater adhesion properties revealed that the adhesion strength was still maintained at 2.56 kPa after soaking the pig skin adhering with α-CD/C9-PVA films in water for 12 h (Figure S8b), while PVA films with poor water resistance dissolved into small pieces (Figure S10). α-CD/C9-PVA electrodes deposited with the Ag NW network were rinsed under a water stream, and a stable ECG waveform could still be recorded after 15 min, while the commercial gel electrode had missing signal due to the decrease in adhesion with the existence of a water film (Figure 4h).

In addition, we wear the electrodes for 1 day to test the interface contact impedance every 1 h as shown in Figure S11. Low impedance can be maintained on the interface at low frequencies (10−100 Hz), which shows that our electrode maintains excellent performance for a long time.

EMG Signal Monitoring. The basic noise level with muscles relaxing has a major role in the total noise in EMG electrical activity.[48] The baseline potential from commercial electrodes and CCP/glycerol electrodes was recorded under the condition of motionless and shaking arms, and the RMS was calculated to compare the noise level. CCP/glycerol electrodes (25.9 and 25.4 μV) exhibited lower noise levels than Ag/AgCl gel electrodes (32.9 and 29.5 μV) (Figure S12), which assured stronger anti-interference levels in EMG signal recording. Moreover, CCP/glycerol electrodes exhibited a more stable power distribution from the time−frequency diagram. In general, the abovementioned results showed that our electrodes meet the requirements for the following EMG signal collection. When recording EMG signals, the following actions were executed: (1) making a fist and extending the palm, and (2) extending five fingers, which were extensively adopted in gesture recognition. Statistical RMS values were extracted to compare EMG signals simulated by different

https://doi.org/10.1021/acsami.1c23322
ACS Appl. Mater. Interfaces 2022, 14, 12812−12823

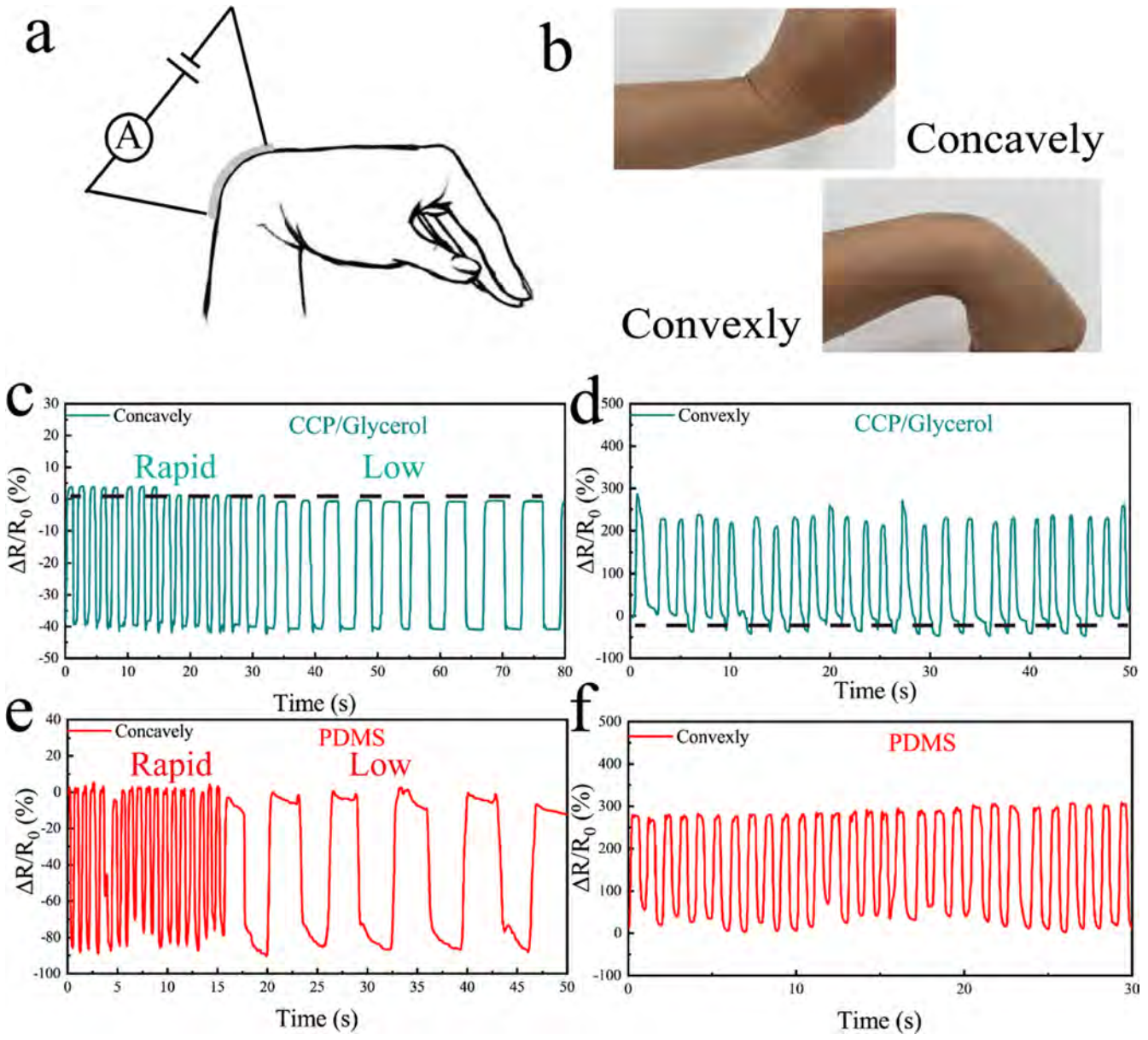

Figure 6. (a) Schematic diagram of the strain sensor/adhesive substrate monitoring the bending direction of the wrist. (b) Photos of the strain sensor on the skin. CCP/glycerol−Ag NW sensors and PDMS−Ag NW sensors (fixed using adhesive tape) are attached to the skin for the resistance change test of different movements. (c,e) Curl inward. (d,f) Stretch outward.

electrodes under the conditions of making a fist and extending the palm (Figure 5a,b). It is indicated that CCP/glycerol electrodes exhibited more differentiated characteristic parameters (RMS_{Fist}/RMS_{Palm}) to be more favorable for gesture distinguishing (Figure 5c). The energy density distribution recorded during continuous motions further proved the feasibility of monitoring EMG signals (Figure 5d). What is more, the SNR of our electrodes corresponding to different actions is higher than that of Ag/AgCl gel electrodes (Figure 5e). The EMG signals of extending five fingers present different amplitudes and duration times (Figure 5f). A mean power frequency was extracted to distinguish different gestures (Figure 5g), which lays the foundation for the human−computer interaction.

Strain-Sensing Test at the Wrist. The conformal contact between the skin and stretchable strain sensors is also significant for motion monitoring, which plays an essential role in transferring strain of the skin to the strain sensor.[49,50] The traditional method to fix PDMS-based strain sensors onto the skin is by using tapes, which is not stable and can cause irritation for long-term use. Notably, CCP/glycerol-based strain sensors presented smaller noise in signals than nonadhesive strain sensors (PDMS) under large strain deformations (Figure 6), especially for the motion of bending wrists concavely at a low frequency, as shown in Figure 6c,e, which originated from uniform strain confirmed by conformal match with the skin and is advantageous for monitoring the direction of wrist movement.

CONCLUSIONS

In summary, CCP/glycerol films with high adhesion strength (6.3 kPa), low elastic modulus (5 MPa), and high air permeability (726 g m^{-2} d^{-1}) were obtained by grafting nonyl groups onto PVA chains and with the addition of

https://doi.org/10.1021/acsami.1c23322
ACS Appl. Mater. Interfaces 2022, 14, 12812−12823

glycerol. The good mechanical and biocompatible properties of the substrate ensured its feasibility in stable ECG recording even under skin mechanical deformation and a sweating state. The EMG signals of different actions can also be acquired to realize the distinction between gestures. The newly adhesive substrate can be used as a medium for the skin to transmit force to the sensitive layer. Considering the low cost and the high performance, the electrode shows potential in a wide application of long-term wireless health monitoring and human−computer interaction.

EXPERIMENTAL SECTION

Materials. PVA (degree of alcoholysis: 87.0−89.0 purity 1788), dimethyl sulfoxide (DMSO, GC, ≥99.0%), and glycerol (99%) were purchased from Greagent (Shanghai Titan Scientific Co., Ltd.). Hydrochloric acid (HCl, 40 wt %, AR) was purchased from China National Medicines Corporation Ltd. Nonanal (95%) and α-CD (98% +) were obtained from Adamas (Shanghai Titan Scientific Co., Ltd.). The Ag NW ethanol solution (10 mg/mL, average diameter of 120 nm, length of 20 μm) was purchased from XFNANO Corporation. Dilute it to 1 mg/mL in ethanol when spraying.

Synthesis of C9-PVA. Modified PVA was synthesized by the homogeneous method reported previously,[31,S1] 10 g of PVA particles (0.05 g/mL) were dissolved in a mixture of deionized water and DMSO (1:3 V/V). Then, the mixture was thermostated at 90 °C for 1 h in an oil bath with HCl (1 mol/L) as a catalyst. Afterward, 1.62 g of nonanal was added dropwise to the mixed solution, keeping the reaction stirring for 1 h at 50 °C. 600 mL of cold ethanol was added to wash away DMSO and unreacted nonanal after the reaction finished. Finally, the C9-PVA precipitated was collected and dried under a vacuum for 24 h (C9-PVA means PVA grafted with a nonyl group).

Preparation of α-CD/C9-PVA/Glycerol Electrodes. α-CD/C9-PVA/glycerol electrodes were prepared using the following steps. First, the suspension containing C9-PVA powder (10 mg/mL) and α-CD (5 mg/mL) dissolved in 40% ethanol was reacted in an autoclave at 90 °C for 10 min. The mixture can be stable for a long time. Then, the mixture, with the addition of the glycerol solution (28 wt %), was stirred for 2 h and was cast in a designated mold at 80 °C for 5 h to finally form the adhesive film. The last step to fabricating the electrode involved the spray coating of silver NWs using the Cordless Airbrush System to form a conductive layer. Briefly, 9 mL of the Ag NW ethanol solution (1 mg/mL) was sprayed onto the CCP/glycerol film for 5 min, keeping the film on the hot plate with the temperature at 80 °C. The distance between the nozzle and the hot stage is 13 cm, and the working pressure and the air flow are 25 PSI and 7 L/min, respectively.

Characterization. SEM images were used to characterize the morphologies of films (SU8200, Hitachi, Japan). The molecular structure was analyzed by FT-IR spectroscopy (iN10 iZ10, Thermofisher, America). The surface hydrophilicity was characterized by the water contact angle of the films (OCA25, Dataphysics, Germany). The crystallization of polymer films was analyzed using a high-resolution X-ray diffractometer (D8 Discover Davinci, Bruker AXS GmbH, Germany). The stress−strain measurements were conducted by using a universal testing machine (CMT6103, MTS Systems China) at a strain rate of 5 mm/min. In a characterization of tensile adhesion tests, 40 μL of the 40% ethanol solution was first sprayed on the skin. Then, a T-shaped mold (3 cm × 3 cm × 0.5 cm) glued with the film was fixed on the testing machine, and the test was measured with the laminating film on the skin at an applied force of 3 N, duration of 6 min, and a rate of 10 mm/min. The interface contact impedance was carried out by an electrochemical workstation (Autolab) with an applied potential of 100 mV and a frequency window from 0.1 Hz to 100 kHz. Two 1.2 cm diameter electrodes were mounted onto the forearm skin with a center distance of 4 cm. Air permeability was measured by the weight change of water in a glass bottle after being sealed with the film for 7 days. The humidity of the test environment is 75% RH and the temperature is 25 °C.

Electrophysiological Signal Test. All the samples were circular electrodes with an area of 4 cm^2 for electrophysiological signal testing. The ECG signals of the volunteer under different states were recorded using the cardiac monitoring apparatus (PC-80B, Healforce, China). A positive electrode playing the role of a reference electrode was placed on the left lower limb. Two other electrodes served as working electrodes and were mounted on the left upper limb and the right upper limb according to the positioning system of limb leads. EMG signals were collected with a sampling frequency of 1000 Hz (ZJE-II, China). The attachment position of the surface EMG electrode corresponding to different muscle tissues will affect the signal amplitude, so the electrodes were placed in the same position. The electrodes are attached to the forearm at an interval of 2 cm, and the corresponding muscle is the total extensor muscle.

The procedure for placing the electrode on the skin and connecting the electrode with the devices has been presented as follows. First, the electrode and the equipment were connected by the following methods. When the electrode is prepared, one end of the copper conductive tape is adhered to the edge of the electrode through silver slurry. In order to prevent the influence of the copper conductive tape during the test, the side close to the skin should be sealed using the insulating tape. Second, the adhering of the electrodes onto the skin and the testing procedures for ECG and EMG are as follows. Spray 40% EtOH on the surface of the skin, then place the electrode on the water mist and press it until water completely evaporates. During the specific test, connect one end of the equipment with the copper conductive tape. Stress concentration caused by modulus mismatch between the electrode and the copper conductive tape and the pulling of the nonadhesive copper may damage the electrode. Thus, in order to prevent the interference caused by wire shaking and connector damage, fix the copper on the skin using the 3M tape.

SNR Calculation Method. The SNR is calculated by the following method. First, Welch's method was adapted to estimate the power spectral density. The arguments to the pwelch function were selected to be a 1024-point Hanning window, a 10240-point nfft, and a 50% overlap. Then, the power of the signal (P_n) was acquired from the region below 100 Hz and the power of noise (P_s) was acquired from 200−300 Hz. Finally, we can calculate the SNR using the following formula

$$\mathrm{SNR} = 10 \times \log_{10}\left(\frac{P_s}{P_n}\right) \quad (1)$$

ASSOCIATED CONTENT

Supporting Information

The Supporting Information is available free of charge at https://pubs.acs.org/doi/10.1021/acsami.1c23322.

XRD, SEM images, cyclic stress−strain test, adhesion strength test, and resistance and T-Peel strength test of different PVA-based films; theoretical calculation of electrode/skin interfacial conformability; interface contact impedance between PVA electrodes or CCP/glycerol electrodes and the skin in different conditions; healing process of the film under the action of external conditions; influence of different modification conditions on the water resistance of the film; baseline EMG signals recorded by different electrodes; and performance comparison of the CCP/glycerol film and representative reported materials (PDF).

ECG signals during walking for an hour (MP4)

https://doi.org/10.1021/acsami.1c23322
ACS Appl. Mater. Interfaces 2022, 14, 12812−12823

AUTHOR INFORMATION

Corresponding Authors

Ranran Wang − *The State Key Laboratory of High Performance Ceramics and Superfine Microstructure, Shanghai Institute of Ceramics, Chinese Academy of Science, Shanghai 200050, China; School of Chemistry and Materials Science, Hangzhou Institute for Advanced Study, University of Chinese Academy of Sciences, Hangzhou 310024, China*; Phone: +86-21-69163759; Email: wangranran@mail.sic.ac.cn

Jing Sun − *The State Key Laboratory of High Performance Ceramics and Superfine Microstructure, Shanghai Institute of Ceramics, Chinese Academy of Science, Shanghai 200050, China*; orcid.org/0000-0003-1101-1584; Phone: +86-21-69163759; Email: jingsun@mail.sic.ac.cn

Authors

Yan Liu − *The State Key Laboratory of High Performance Ceramics and Superfine Microstructure, Shanghai Institute of Ceramics, Chinese Academy of Science, Shanghai 200050, China; University of Chinese Academy of Sciences, Beijing 100049, China*

Yin Cheng − *The State Key Laboratory of High Performance Ceramics and Superfine Microstructure, Shanghai Institute of Ceramics, Chinese Academy of Science, Shanghai 200050, China*

Liangjing Shi − *The State Key Laboratory of High Performance Ceramics and Superfine Microstructure, Shanghai Institute of Ceramics, Chinese Academy of Science, Shanghai 200050, China*

Complete contact information is available at: https://pubs.acs.org/10.1021/acsami.1c23322

Author Contributions

J.S. and R.W. conceptualized the project. Y.L. and R.W. planned and designed the experiments. Y.L. and R.W. performed the experiments, analyzed the data, and wrote the paper. Y.C. helped to do data analysis. L.S. and Y.C. helped to do experiments. All the authors have approved the final version of the manuscript. J.S. supervised the project.

Notes

The authors declare no competing financial interest.

ACKNOWLEDGMENTS

This work was supported by the Youth Innovation Promotion Association CAS (Y201841); the National Natural Science Foundation of China (61871368 and 62122080); the Austrian-Chinese Cooperative Research and Development projects (GJHZ2046 and POWERTEX); and the Instrument and equipment development program sponsored by CAS (YJ-KYYQ20180065).

ABBREVIATIONS

ECG, electrocardiogram
EMG, electromyogram
WVTR, water vapor transmission rate
RMS, root mean square
SNR, signal-to-noise ratio
PVA, polyvinyl alcohol
C9-PVA, represents PVA molecules grafted with nonyl
α-CD/C9-PVA, represents the mixture of α-cyclodextrin and C9-PVA
α-CD/C9-PVA/glycerol (CCP/glycerol), represents the mixture of α-CD/C9-PVA and glycerol

REFERENCES

(1) Gao, D.; Parida, K.; Lee, P. S. Emerging Soft Conductors for Bioelectronic Interfaces. *Adv. Funct. Mater.* **2019**, *30*, 1907184.

(2) Yang, Y.; Shi, L.; Cao, Z.; Wang, R.; Sun, J. Strain Sensors with a High Sensitivity and a Wide Sensing Range Based on a Ti3c2tx-(Mxene) Nanoparticle−Nanosheet Hybrid Network. *Adv. Funct. Mater.* **2019**, *29*, 1807882.

(3) Lee, H.; Choi, T. K.; Lee, Y. B.; Cho, H. R.; Ghaffari, R.; Wang, L.; Choi, H. J.; Chung, T. D.; Lu, N.; Hyeon, T.; Choi, S. H.; Kim, D.-H. A Graphene-Based Electrochemical Device with Thermoresponsive Microneedles for Diabetes Monitoring and Therapy. *Nat. Nanotechnol.* **2016**, *11*, 566−572.

(4) Gao, W.; Emaminejad, S.; Nyein, H. Y. Y.; Challa, S.; Chen, K.; Peck, A.; Fahad, H. M.; Ota, H.; Shiraki, H.; Kiriya, D.; Lien, D.-H.; Brooks, G. A.; Davis, R. W.; Javey, A. Fully Integrated Wearable Sensor Arrays for Multiplexed in Situ Perspiration Analysis. *Nature* **2016**, *529*, 509.

(5) Cea, C.; Spyropoulos, G. D.; Jastrzebska-Perfect, P.; Ferrero, J. J.; Gelinas, J. N.; Khodagholy, D. Enhancement-Mode Ion-Based Transistor as a Comprehensive Interface and Real-Time Processing Unit for in Vivo Electrophysiology. *Nat. Mater.* **2020**, *19*, 679−686.

(6) Xu, B.; Akhtar, A.; Liu, Y.; Chen, H.; Yeo, W.-H.; Park, S. I.; Boyce, B.; Kim, H.; Yu, J.; Lai, H.-Y.; Jung, S.; Zhou, Y.; Kim, J.; Cho, S.; Huang, Y.; Bretl, T.; Rogers, J. A. An Epidermal Stimulation and Sensing Platform for Sensorimotor Prosthetic Control, Management of Lower Back Exertion, and Electrical Muscle Activation. *Adv. Mater.* **2016**, *28*, 4462−4471.

(7) Sun, B.; McCay, R. N.; Goswami, S.; Xu, Y.; Zhang, C.; Ling, Y.; Lin, J.; Yan, Z. Gas-Permeable, Multifunctional on-Skin Electronics Based on Laser-Induced Porous Graphene and Sugar-Templated Elastomer Sponges. *Adv. Mater.* **2018**, *30*, 1804327.

(8) Jang, K.-I.; Han, S. Y.; Xu, S.; Mathewson, K. E.; Zhang, Y.; Jeong, J.-W.; Kim, G.-T.; Webb, C.; Lee, J. W.; Dawidczyk, T. J.; Kim, R. H.; Song, Y. M.; Yeo, W.-H.; Kim, S.; Cheng, H.; Il Rhee, S.; Chung, J.; Kim, B.; Chung, H. U.; Lee, D.; Yang, Y.; Cho, M.; Gaspar, J. G.; Carbonari, R.; Fabiani, M.; Gratton, G.; Huang, Y.; Rogers, J. A. Rugged and Breathable Forms of Stretchable Electronics with Adherent Composite Substrates for Transcutaneous Monitoring. *Nat. Commun.* **2014**, *5*, 4779−10.

(9) Yamamoto, Y.; Harada, S.; Yamamoto, D.; Honda, W.; Arie, T.; Akita, S.; Takei, K. Printed Multifunctional Flexible Device with an Integrated Motion Sensor for Health Care Monitoring. *Sci. Adv.* **2016**, *2*, No. e1601473.

(10) Norton, J. J. S.; Lee, D. S.; Lee, J. W.; Lee, W.; Kwon, O.; Won, P.; Jung, S.-Y.; Cheng, H.; Jeong, J.-W.; Akce, A.; Umunna, S.; Na, I.; Kwon, Y. H.; Wang, X.-Q.; Liu, Z.; Paik, U.; Huang, Y.; Bretl, T.; Yeo, W.-H.; Rogers, J. A. Soft, Curved Electrode Systems Capable of Integration on the Auricle as a Persistent Brain-Computer Interface. *Proc. Natl. Acad. Sci. U.S.A.* **2015**, *112*, 3920−3925.

(11) Moin, A.; Zhou, A.; Rahimi, A.; Menon, A.; Benatti, S.; Alexandrov, G.; Tamakloe, S.; Ting, J.; Yamamoto, N.; Khan, Y.; Burghardt, F.; Benini, L.; Arias, A. C.; Rabaey, J. M. A Wearable Biosensing System with in-Sensor Adaptive Machine Learning for Hand Gesture Recognition. *Nat. Electron.* **2020**, *4*, 54−63.

(12) Wang, M.; Wang, T.; Luo, Y.; He, K.; Pan, L.; Li, Z.; Cui, Z.; Liu, Z.; Tu, J.; Chen, X. Fusing Stretchable Sensing Technology with Machine Learning for Human−Machine Interfaces. *Adv. Funct. Mater.* **2021**, *31*, 2008807.

(13) Stark, G.; Huber, U.; Hofer, E. Continuous Ecg Measurements of Intracardiac Activity from the Surface of Langendorff-Perfused Guinea Pig Hearts. *Basic Res. Cardiol.* **1987**, *82*, 437−444.

(14) Jo, M.; Min, K.; Roy, B.; Kim, S.; Lee, S.; Park, J. Y.; Kim, S. Protein-Based Electronic Skin Akin to Biological Tissues. *ACS Nano* **2018**, *12*, 5637−5645.

(15) Kim, D. H.; Lu, N.; Ma, R.; Kim, Y. S.; Kim, R. H.; Wang, S.; Wu, J.; Won, S. M.; Tao, H.; Islam, A.; Yu, K. J.; Kim, T. I.;

Chowdhury, R.; Ying, M.; Xu, L.; Li, M.; Chung, H. J.; Keum, H.; McCormick, M.; Liu, P.; Zhang, Y. W.; Omenetto, F. G.; Huang, Y.; Coleman, T.; Rogers, J. A. Epidermal Electronics. *Science* **2011**, *333*, 838−843.
(16) Khan, Y.; Garg, M.; Gui, Q.; Schadt, M.; Gaikwad, A.; Han, D.; Yamamoto, N. A. D.; Hart, P.; Welte, R.; Wilson, W.; Czarnecki, S.; Poliks, M.; Jin, Z.; Ghose, K.; Egitto, F.; Turner, J.; Arias, A. C. Flexible Hybrid Electronics: Direct Interfacing of Soft and Hard Electronics for Wearable Health Monitoring. *Adv. Funct. Mater.* **2016**, *26*, 8764−8775.
(17) Kabiri Ameri, S.; Ho, R.; Jang, H.; Tao, L.; Wang, Y.; Wang, L.; Schnyer, D. M.; Akinwande, D.; Lu, N. Graphene Electronic Tattoo Sensors. *ACS Nano* **2017**, *11*, 7634−7641.
(18) Kireev, D.; Okogbue, E.; Jayanth, R. T.; Ko, T. J.; Jung, Y.; Akinwande, D. Multipurpose and Reusable Ultrathin Electronic Tattoos Based on Ptse2 and Ptte2. *ACS Nano* **2021**, *15*, 2800−2811.
(19) Chae, H.; Kwon, H. J.; Kim, Y. K.; Won, Y.; Kim, D.; Park, H. J.; Kim, S.; Gandla, S. Laser-Processed Nature-Inspired Deformable Structures for Breathable and Reusable Electrophysiological Sensors toward Controllable Home Electronic Appliances and Psychophysiological Stress Monitoring. *ACS Appl. Mater. Interfaces* **2019**, *11*, 28387−28396.
(20) Wang, S.; Li, M.; Wu, J.; Kim, D.-H.; Lu, N.; Su, Y.; Kang, Z.; Huang, Y.; Rogers, J. A. Mechanics of Epidermal Electronics. *J. Appl. Mech.* **2012**, *79*, 031022−31031.
(21) Yang, X.; Li, L.; Wang, S.; Lu, Q.; Bai, Y.; Sun, F.; Li, T.; Li, Y.; Wang, Z.; Zhao, Y.; Shi, Y.; Zhang, T. Ultrathin, Stretchable, and Breathable Epidermal Electronics Based on a Facile Bubble Blowing Method. *Adv. Electron. Mater.* **2020**, *6*, 2000306.
(22) Wang, Y.; Lee, S.; Wang, H.; Jiang, Z.; Jimbo, Y.; Wang, C.; Wang, B.; Kim, J. J.; Koizumi, M.; Yokota, T.; Someya, T. Robust, Self-Adhesive, Reinforced Polymeric Nanofilms Enabling Gas-Permeable Dry Electrodes for Long-Term Application. *Proc. Natl. Acad. Sci. U.S.A.* **2021**, *118*, No. e2111904118.
(23) Xu, Y.; Sun, B.; Ling, Y.; Fei, Q.; Chen, Z.; Li, X.; Guo, P.; Jeon, N.; Goswami, S.; Liao, Y.; Ding, S.; Yu, Q.; Lin, J.; Huang, G.; Yan, Z. Multiscale Porous Elastomer Substrates for Multifunctional on-Skin Electronics with Passive-Cooling Capabilities. *Proc. Natl. Acad. Sci. U.S.A.* **2020**, *117*, 205−213.
(24) Kim, J. H.; Kim, S. R.; Kil, H. J.; Kim, Y. C.; Park, J. W. Highly Conformable, Transparent Electrodes for Epidermal Electronics. *Nano Lett.* **2018**, *18*, 4531−4540.
(25) Xu, Z.; Chen, L.; Lu, L.; Du, R.; Ma, W.; Cai, Y.; An, X.; Wu, H.; Luo, Q.; Xu, Q.; Zhang, Q.; Jia, X. A Highly-Adhesive and Self-Healing Elastomer for Bio-Interfacial Electrode. *Adv. Funct. Mater.* **2020**, *31*, 2006432.
(26) Ye, G.; Qiu, J.; Fang, X.; Yu, T.; Xie, Y.; Zhao, Y.; Yan, D.; He, C.; Liu, N. A Lamellibranchia-Inspired Epidermal Electrode for Electrophysiology. *Mater. Horiz.* **2021**, *8*, 1047−1057.
(27) Liang, Y.; He, J.; Guo, B. Functional Hydrogels as Wound Dressing to Enhance Wound Healing. *ACS Nano* **2021**, *15*, 12687−12722.
(28) Liu, Y.; Zhang, Q.; Zhou, N.; Tan, J.; Ashley, J.; Wang, W.; Wu, F.; Shen, J.; Zhang, M. Study on a Novel Poly (Vinyl Alcohol)/Graphene Oxide-Citicoline Sodium-Lanthanum Wound Dressing: Biocompatibility, Bioactivity, Antimicrobial Activity, and Wound Healing Effect. *Chem. Eng. J.* **2020**, *395*, 125059.
(29) Abdullah, Z. W.; Dong, Y. Preparation and Characterisation of Poly(Vinyl) Alcohol (Pva)/Starch (St)/Halloysite Nanotube (Hnt) Nanocomposite Films as Renewable Materials. *J. Mater. Sci.* **2017**, *53*, 3455−3469.
(30) Yang, H.; Ji, S.; Chaturvedi, I.; Xia, H.; Wang, T.; Chen, G.; Pan, L.; Wan, C.; Qi, D.; Ong, Y.-S.; Chen, X. Adhesive Biocomposite Electrodes on Sweaty Skin for Long-Term Continuous Electrophysiological Monitoring. *ACS Mater. Lett.* **2020**, *2*, 478−484.
(31) Chen, X.; Taguchi, T. Enhanced Skin Adhesive Property of Hydrophobically Modified Poly(Vinyl Alcohol) Films. *ACS Omega* **2020**, *5*, 1519−1527.
(32) Tretinnikov, O. N.; Zagorskaya, S. A. Determination of the Degree of Crystallinity of Poly (Vinyl Alcohol) by Ftir Spectroscopy. *J. Appl. Spectrosc.* **2012**, *79*, 521−526.
(33) Fan, H.; Wang, J.; Gong, J. P. Barnacle Cement Proteins-Inspired Tough Hydrogels with Robust, Long-Lasting, and Repeatable Underwater Adhesion. *Adv. Funct. Mater.* **2020**, *31*, 202009334.
(34) Ershad, F.; Thukral, A.; Yue, J.; Comeaux, P.; Lu, Y.; Shim, H.; Sim, K.; Kim, N. I.; Rao, Z.; Guevara, R.; Contreras, L.; Pan, F.; Zhang, Y.; Guan, Y. S.; Yang, P.; Wang, X.; Wang, P.; Wu, X.; Yu, C. Ultra-Conformal Drawn-on-Skin Electronics for Multifunctional Motion Artifact-Free Sensing and Point-of-Care Treatment. *Nat. Commun.* **2020**, *11*, 3823.
(35) Zhang, L.; Kumar, K. S.; He, H.; Cai, C. J.; He, X.; Gao, H.; Yue, S.; Li, C.; Seet, R. C.; Ren, H.; Ouyang, J. Fully Organic Compliant Dry Electrodes Self-Adhesive to Skin for Long-Term Motion-Robust Epidermal Biopotential Monitoring. *Nat. Commun.* **2020**, *11*, 4683.
(36) Yu, B.; Kang, S. Y.; Akthakul, A.; Ramadurai, N.; Pilkenton, M.; Patel, A.; Nashat, A.; Anderson, D. G.; Sakamoto, F. H.; Gilchrest, B. A.; Anderson, R. R.; Langer, R. An Elastic Second Skin. *Nat. Mater.* **2016**, *15*, 911−918.
(37) Woo, E. J.; Hua, P.; Webster, J. G.; Tompkins, W. J.; Pallas-Areny, R. Skin Impedance Measurements Using Simple and Compound Electrodes. *Med. Biol. Eng. Comput.* **1992**, *30*, 97−102.
(38) Pan, L.; Cai, P.; Mei, L.; Cheng, Y.; Zeng, Y.; Wang, M.; Wang, T.; Jiang, Y.; Ji, B.; Li, D.; Chen, X. A Compliant Ionic Adhesive Electrode with Ultralow Bioelectronic Impedance. *Adv. Mater.* **2020**, *32*, No. e2003723.
(39) Seo, J.-W.; Kim, H.; Kim, K.; Choi, S. Q.; Lee, H. J. Calcium-Modified Silk as a Biocompatible and Strong Adhesive for Epidermal Electronics. *Adv. Funct. Mater.* **2018**, *28*, 1800802.
(40) de Talhouet, H.; Webster, J. G. The Origin of Skin-Stretch-Caused Motion Artifacts under Electrodes. *Physiol. Meas.* **1996**, *17*, 81−93.
(41) Miyamoto, A.; Lee, S.; Cooray, N. F.; Lee, S.; Mori, M.; Matsuhisa, N.; Jin, H.; Yoda, L.; Yokota, T.; Itoh, A.; Sekino, M.; Kawasaki, H.; Ebihara, T.; Amagai, M.; Someya, T. Inflammation-Free, Gas-Permeable, Lightweight, Stretchable on-Skin Electronics with Nanomeshes. *Nat. Nanotechnol.* **2017**, *12*, 907−913.
(42) Jeong, J. W.; Kim, M. K.; Cheng, H.; Yeo, W. H.; Huang, X.; Liu, Y.; Zhang, Y.; Huang, Y.; Rogers, J. A. Capacitive Epidermal Electronics for Electrically Safe, Long-Term Electrophysiological Measurements. *Adv. Healthcare Mater.* **2014**, *3*, 642−648.
(43) Spence, K. L.; Venditti, R. A.; Rojas, O. J.; Pawlak, J. J.; Hubbe, M. A. Water Vapor Barrier Properties of Coated and Filled Microfibrillated Cellulose Composite Films. *BioResources* **2011**, *6*, 4370−4388.
(44) Abdullah, Z. W.; Dong, Y.; Davies, I. J.; Barbhuiya, S. Pva, Pva Blends and Their Nanocomposites for Biodegradable Packaging Application. *Polym.-Plast. Technol. Eng. Polym.* **2017**, *56*, 1307−1344.
(45) Kim, J. W.; Park, H.; Lee, G.; Jeong, Y. R.; Hong, S. Y.; Keum, K.; Yoon, J.; Kim, M. S.; Ha, J. S. Paper-Like, Thin, Foldable, and Self-Healable Electronics Based on Pva/Cnc Nanocomposite Film. *Adv. Funct. Mater.* **2019**, *29*, 1905968.
(46) Cameron, J. Bioelectromagnetism—Principles and Applications of Bioelectric and Biomagnetic Fields. *Med. Phys.* **1996**, *23*, 1471.
(47) Liao, L. D.; Wang, I. J.; Chen, S. F.; Chang, J. Y.; Lin, C. T. Design, Fabrication and Experimental Validation of a Novel Dry-Contact Sensor for Measuring Electroencephalography Signals without Skin Preparation. *Sensors* **2011**, *11*, 5819−5834.
(48) Huigen, E.; Peper, A.; Grimbergen, C. A. Investigation into the Origin of the Noise of Surface Electrodes. *Med. Biol. Eng. Comput.* **2002**, *40*, 332−338.
(49) Liu, X.; Liu, J.; Wang, J.; Wang, T.; Jiang, Y.; Hu, J.; Liu, Z.; Chen, X.; Yu, J. Bioinspired, Microstructured Silk Fibroin Adhesives for Flexible Skin Sensors. *ACS Appl. Mater. Interfaces* **2020**, *12*, 5601−5609.
(50) Wang, S.; Fang, Y.; He, H.; Zhang, L.; Li, C. a.; Ouyang, J. Wearable Stretchable Dry and Self-Adhesive Strain Sensors with

Conformal Contact to Skin for High-Quality Motion Monitoring. *Adv. Funct. Mater.* **2020**, *31*, 2007495.
(51) Chen, X.; Taguchi, T. Enhanced Skin Adhesive Property of Alpha-Cyclodextrin/Nonanyl Group-Modified Poly(Vinyl Alcohol) Inclusion Complex Film. *Carbohydr. Polym.* **2021**, *263*, 117993.

https://doi.org/10.1021/acsami.1c23322
ACS Appl. Mater. Interfaces 2022, 14, 12812−12823